AAC
Journals.ASM.org

A Novel Inhibitor of Dengue Virus Replication That Targets the Capsid Protein

Chelsea M. Byrd,[a] Dongcheng Dai,[a] Douglas W. Grosenbach,[a] Aklile Berhanu,[a] Kevin F. Jones,[a] Kara B. Cardwell,[a] Christine Schneider,[a] Kristin A. Wineinger,[a] Jessica M. Page,[a] Chris Harver,[a] Eric Stavale,[a] Shanthakumar Tyavanagimatt,[a] Melialani A. Stone,[a] Ralf Bartenschlager,[b] Pietro Scaturro,[b] Dennis E. Hruby,[a] Robert Jordan[a]*

SIGA Technologies, Inc., Corvallis, Oregon, USA,[a] Department of Infectious Diseases, Molecular Virology, University of Heidelberg, Heidelberg, Germany[b]

Dengue viruses (DENV) infect 50 to 100 million people worldwide per year, of which 500,000 develop severe life-threatening disease. This mosquito-borne illness is endemic in most tropical and subtropical countries and has spread significantly over the last decade. While there are several promising vaccine candidates in clinical trials, there are currently no approved vaccines or therapeutics available for treatment of dengue infection. Here, we describe a novel small-molecule compound, ST-148, that is a potent inhibitor of all four serotypes of DENV *in vitro*. ST-148 significantly reduced viremia and viral load in vital organs and tended to lower cytokine levels in the plasma in a nonlethal model of DENV infection in AG129 mice. Compound resistance mapped to the DENV capsid (C) gene, and a direct interaction of ST-148 with C protein is suggested by alterations of the intrinsic fluorescence of the protein in the presence of compound. Thus, ST-148 appears to interact with the DENV C protein and inhibits a distinct step(s) of the viral replication cycle.

Dengue fever (DF) is an acute, febrile illness caused by infection with dengue virus (DENV). DENV circulates in populations as one of four distinct serotypes and is transmitted to humans via the bite of the *Aedes* mosquito. While DF is a debilitating illness, most cases resolve without sequelae (1). In a small percentage of cases, individuals develop a severe capillary leakage syndrome, referred to as dengue hemorrhagic fever (DHF), which can lead to a more severe disease called dengue shock syndrome (DSS) (1, 2). An estimated 50 to 100 million individuals are infected with DENV each year, mostly in tropical and subtropical areas of southeast Asia, resulting in nearly 500,000 severe life-threatening illnesses and 25,000 deaths. The incidence of dengue disease is growing as the mosquito vector spreads due to urbanization, population growth, increased international travel, a decrease in mosquito control efforts, and global warming (3).

The existence of four distinct serotypes has made DENV vaccine development challenging. While serotype-specific immunity reduces the rate of reinfection, immunity does not provide complete protection from infection by the other three virus serotypes (4). In fact, a second infection with a different virus serotype can increase the risk of severe disease. This enhanced risk is thought to be due to a combination of viral genetics and heterotypic, nonneutralizing antibodies which enhance virus infection (5). Disease severity has been linked to viral load, and patients with DHF or DSS have viral titers in the blood that are 10- to 1,000-fold-higher than in patients with DF (6). Thus, an antiviral drug administered early during the course of infection that inhibits viral replication and decreases viral load might be expected to reduce the severity of disease.

DENV belongs to the *Flaviviridae* family and can be cultured in several transformed cell lines to produce robust cytopathic effects. Upon entry of the virus into the host cell, the positive, single-stranded RNA genome is translated into a single polyprotein that is proteolytically processed to produce three structural proteins, capsid (C), premembrane (prM), and envelope (E), and seven nonstructural proteins, NS1, NS2A, NS2B, NS3, NS4A, NS4B, and NS5. The nonstructural proteins form the viral replicase that is found within vesicles derived from virus-modified endoplasmic reticulum (ER) membranes (7). Full-length, positive-stranded viral RNA genomes are synthesized from a negative-stranded intermediate (8). The newly synthesized RNA genomes are thought to exit through pores that connect the vesicles to the cytosol (7). The viral core (C) protein associates with the genomic RNA to form the nucleocapsid, which buds into the ER lumen to produce the immature virus particle containing viral prM and E glycoproteins (9). The immature virus particles traffic via the secretory pathway and are processed in the late Golgi compartment by a furin protease that cleaves the prM protein to produce infectious virus particles that are released from the cell (10, 11).

A number of antiviral compounds have been identified that inhibit DENV replication *in vitro* and *in vivo* (reviewed in reference 12). Virus-specific inhibitors have been identified that target the viral envelope (13), methyl transferase (14), protease (15), NS4B protein (16), polymerase (17, 18), and virus-specific RNA translation (19). In addition, compounds that target host enzymes, such as ER glucosidases (20–23), dihydroorotate dehydrogenase (19), and an intracellular cholesterol transporter (24), have been shown to have antiviral activity. Although these compounds appear to be effective at inhibiting DENV replication, there is still no approved antiviral therapeutic for the treatment of DENV infection in humans.

To identify potential antiviral therapeutics to treat DENV infection, a high-throughput screening (HTS) assay was developed that measured virus-induced cytopathic effects (CPE). This assay

Received 11 July 2012 **Returned for modification** 3 August 2012
Accepted 26 September 2012
Published ahead of print 15 October 2012
Address correspondence to Chelsea M. Byrd, cbyrd@siga.com.
* Present address: Robert Jordan, Gilead Sciences, Inc., Foster City, California, USA.

doi:10.1128/AAC.01429-12

was used to screen a chemical compound library composed of over 200,000 unique small molecules to identify inhibitors of DENV replication. A novel compound series with activity against all four DENV serotypes was identified. The lead compound in this series, ST-148, inhibited DENV replication in multiple cell types and reduced viral load in a mouse model of DENV replication. Drug resistance was mapped to the capsid coding region of the virus genome, and recombinant DENV containing mutations in this region showed reduced susceptibility to ST-148. The compound altered the intrinsic fluorescence of purified wild-type C protein as well as a mutant C protein containing amino acid changes associated with reduced compound susceptibility. These data suggest that ST-148 inhibits the DENV replication cycle by targeting the C protein.

MATERIALS AND METHODS

Compound synthesis. ST-148 was purchased from ChemBridge (San Diego, CA) and dissolved in dimethyl sulfoxide (DMSO) (Sigma-Aldrich, St. Louis, MO) to a concentration of 10 mM.

Cells and viruses. Vero, BSC40, BHK, C6/36, L929, MDCK, and MDBK cells were obtained from the American Type Culture Collection (ATCC; Manassas, VA), and Huh-7 cells were obtained from the Japan Health Sciences Foundation (Tokyo, Japan). Vero, BSC40, BHK, and L929 cells were maintained at 37°C with 5% CO_2 in minimal essential medium (MEM) supplemented with 10% heat-inactivated fetal bovine serum (FBS), 2 mM L-glutamine, and 10 μg/ml gentamicin (all culture reagents were from Invitrogen, Grand Island, NY). C6/36 cells were maintained at 28°C with 5% CO_2 in MEM as described above. MDBK cells were maintained in MEM as described above and supplemented with 10% horse serum (HS) (Invitrogen) instead of FBS. MDCK cells were maintained in Eagle's modified essential medium (EMEM) (ATCC) with 10% FBS, 100 U/ml penicillin, and 100 μg/ml streptomycin (Invitrogen). Dengue-1 (DENV-1) strain TH-Sman (VR-344), dengue-2 (DENV-2) strain New Guinea C (NGC) (VR-1255), dengue-3 (DENV-3) strain H87 (VR-1256), and dengue-4 (DENV-4) strain H241 (VR-1257) were purchased from ATCC. DENV-2 K0049 was obtained from Rebecca Rico-Hesse (Texas Biomedical Research Institute, San Antonio, TX). DENV-2 S221 was obtained from Sujan Shresta (La Jolla Institute for Allergy and Immunology, La Jolla, CA). The DENV were propagated on Vero or C6/36 cell cultures. Bovine viral diarrhea virus (BVDV) strain NADL (VR-534), Modoc virus strain M544 (VR-415), influenza A virus strain A/PR/8/34 (VR-1469), Sindbis virus strain AR-339 (VR-1585), and herpes simplex virus (HSV) strain KOS (VR-1493) were purchased from the ATCC. Recombinant vaccinia virus expressing green fluorescent protein (vvGFP) is described elsewhere (25). All cell culture incubations, except for C6/36 cell culture, were performed at 37°C with 5% CO_2.

High-throughput screening assay. Vero cell monolayers were seeded on 96-well plates at 4.0×10^3 cells per well and incubated overnight. The cells were then infected with DENV-2 at a multiplicity of infection (MOI) of 0.1 and incubated for 5 days with 5 μM compound added by a Multiprobe II high-throughput system (PerkinElmer, Waltham, MA). Infected cell monolayers were fixed with 5% glutaraldehyde (JT Baker, Central Valley, PA) in phosphate-buffered saline (Fisher, Pittsburgh, PA) and stained with 0.1% crystal violet (Sigma) in 5% methanol for 30 min. Virus-induced cytopathic effects (CPE) were quantified by measuring absorbance at 570 nm on an EnVision multilabel reader (PerkinElmer).

Inhibitory potency. Vero cell monolayers were seeded in 96-well plates at 4.0×10^3 cells per well and incubated overnight. Dose-response curves were generated by measuring virus-induced CPE in the presence of a range of compound concentrations. Eight compound concentrations (25, 8, 2.5, 0.8, 0.25, 0.08, 0.025, and 0.008 μM) were used to generate inhibition curves suitable for calculating the 50% effective concentration (EC50) from virus-induced CPEs. Compound dilutions were prepared in DMSO prior to addition to the cell culture medium. The final DMSO concentration in all samples was 0.5%. Cell monolayers were infected with DENV-2 at an MOI of 0.1. At 5 days postinfection (dpi), the assay was terminated by fixing and staining the cells as described above. The level of CPE was quantified by measuring absorbance at 570 nm. EC_{50}s were calculated by fitting the data to a four-parameter logistic model (variable-slope, nonlinear regression model) to generate a dose-response curve using XLfit 4.1 (IBDS, Emeryville, CA). From this curve, the concentration of compound that inhibited virus-induced CPE by 50% was calculated.

Cytotoxicity assays. For measurement of compound cytotoxicity, Vero, BSC40, and Huh-7 cells were seeded at either 3.5×10^3 or 1.0×10^4 cells per well in MEM supplemented with 5% FBS in 96-well plates, incubated overnight, and then incubated with various concentrations of ST-148 for 48 h. Cell viability was measured using a metabolic activity assay where the absorbance at 570/600 nm was measured on an EnVision multilabel reader at 5 to 6 h after the addition of 470 μM resazurin (Sigma) at 10% of the assay volume and incubation at 37°C with 5% CO_2. BHK cells were seeded at 5.0×10^3 cells per well, and the remainder of the procedure was performed as described above. MDBK cells were seeded at 5.0×10^3 cells per well in MEM supplemented with 2% HS, incubated overnight as described above, and then incubated with various concentrations of ST-148 for 96 h. Cell viability was measured as described above. C6/36 cells were seeded at 4.0×10^4 cells per well, incubated overnight at 28°C with 5% CO_2, and then incubated with various concentrations of ST-148 for 48 h at 28°C with 5% CO_2. Cell viability was measured as described above. For the 5-day cytotoxicity assay, the assay was performed as described above with the following modifications: Vero cells were seeded at 3.5×10^3 cells per well in 96-well plates and incubated for 5 days after compound addition. Cell viability was measured using the Cell Titer Glo luminescent cell viability assay (Promega, Madison, WI) according to the manufacturer's protocol. Luminescence was measured on an EnVision multilabel reader at 700 nm with a 0.1-s integration time.

Ames assay for genotoxicity. To evaluate the mutagenic potential of ST-148, the compound was tested in the bacterial reverse mutation assay and the Muta-Chromo plate assay (EBPI, Mississauga, Canada). All bacterial tester strains were purchased from Molecular Toxicology, Inc. (Boone, NC). For the bacterial reverse mutation assay, 0.1-ml aliquots of overnight cultures of *E. coli* tester strain WP-2 *uvrA* were added to molten top agar (with 0.5% NaCl, 0.05 mM histidine, and 0.05 mM biotin) in the presence and absence of 10% (vol/vol) Aroclor-1254-induced rat liver S9 (with 0.1 M phosphate buffer, pH 7.4, 4 mM NADP, 6 mM G-6-P, 33 mM $MgCl_2$, and 8 mM KCl) (Molecular Toxicology) and various concentrations of ST-148 with appropriate controls. The top agar mixture was overlaid onto minimal glucose agar plates (Vogel-Bonner medium E with 2% glucose) (Molecular Toxicology), allowed to harden, and incubated at 37°C for 48 to 72 h. After the incubation, any revertant colonies were scored. The Muta-Chromo plate assay was carried out according to the manufacturer's instructions using *Salmonella enterica* serovar Typhimurium tester strains TA-98, TA-100, TA-1535, and TA-1537, Aroclor-1254-induced rat liver S9 with cofactors, and various concentrations of ST-148.

Viral titer reduction assays. A viral titer reduction assay was performed to measure the antiviral efficacy of ST-148 in cell culture. Cells (Vero for DENV or Modoc virus) were seeded at 1×10^5 cells per well in 12-well plates and incubated overnight. Cells were infected with DENV-1, DENV-2, DENV-3, DENV-4, DENV-2 S221, or Modoc virus at an MOI of 0.1 in the presence of various concentrations of ST-148 and incubated for 1.5 h. The inoculum was removed and replaced with MEM supplemented with 2% FBS containing various concentrations of ST-148 and incubated for 48 h. Supernatant was harvested and serially diluted across Vero cells seeded at 3.0×10^5 cells per well in 6-well plates. After a 1.5-h infection, plates were overlaid with a 1:1 mix of SeaPlaque agarose (Lonza, Allendale, NJ) and 2× MEM. Plates were incubated (5 days for Modoc virus, 7 days for DENV-2 and DENV-4, 8 days for DENV-2 S221, and 10 days for DENV-1 and DENV-3). Plates were fixed and stained as described above, with the exception of a shorter stain period (10 s) to visualize plaques.

Time-of-drug-addition assay. One day prior to infection, 3×10^4 Vero cells were seeded in 24-well plates and incubated overnight. Cells were then infected with DENV-2 at an MOI of 1.0. After 1.5 h, the virus inoculum was replaced with MEM supplemented with 1% FBS. ST-148 at a concentration of 25 μM was added to the assay medium at either 2 h prior to infection or at 0 h (i.e., at the time of infection) or 2, 4, 6, 8, 12, 24, or 48 hpi. At 48 hpi the supernatant was harvested and plaque titrated on Vero cells as described above.

Antiviral specificity. All assays (except that for influenza virus) were carried out in the appropriate medium containing 2% FBS (HS for MDBK cells). Ninety-six-well cell culture plates were seeded 24 h prior to use with 2.0×10^4 (Vero for HSV, BSC40 for Sindbis and vvGFP), 1.5×10^4 (Vero for DENV-2 K0049), or 1.0×10^4 (MDBK for BVDV, MDCK for influenza) cells per well. Compound was added to duplicate wells of cells at final concentrations of 50, 25, 12.5, 6.3, 3.1, 1.6, 0.8, and 0 μM. The final concentration of DMSO in the assays was 0.5%. Cells were infected at the cell culture infectious dose causing >90% CPE at 1.6 (Sindbis), 2 (HSV or vvGFP), 3 (influenza), or 4 (BVDV) dpi or at titers that generated an enzyme-linked immunosorbent assay (ELISA) signal of 2.5-fold above the background level for DENV-2 K0049 at the end of the incubation period. For the influenza virus assay, the cell culture medium (EMEM supplemented with 10% FBS and penicillin-streptomycin) was replaced with Ultra MDCK chemically defined, serum-free renal cell medium with L-glutamine (Lonza) containing 5 μg/ml tosylsulfonyl phenylalanyl chloromethyl ketone (TPCK)-treated trypsin (Amersham, Pittsburgh, PA). Influenza virus was added to the culture medium, and virus-induced CPE was measured at 72 h postinfection. As controls, uninfected cells and cells receiving virus without compound were included on each assay plate. At the end of the incubation period, virus-infected cells were fixed and stained as described above. DENV-2 K0049 ELISA was carried out using a 1:100 dilution of mouse monoclonal antibody to DENV prM glycoprotein (Abcam, Cambridge, MA) and a 1:100 dilution of goat anti-mouse IgG (H+L)-horseradish peroxidase conjugate (Bio-Rad, Hercules, CA) as a secondary antibody.

Selection of drug-resistant virus variants. DENV variants with reduced susceptibility to ST-148 were isolated by plating wild-type DENV-2 on Vero cell monolayers in the presence of 5 μM ST-148. The inoculum was removed after 2 h of incubation, replaced with media containing ST-148, and incubated at 37°C with 5% CO_2. At 6 dpi, the supernatant was harvested and applied to Vero cells in the presence of ST-148, and the infection and incubation were repeated as described above. Virus isolates exhibiting reduced susceptibility to ST-148 were plaque purified three times in the presence of compound prior to large-scale stock preparation. The purified virus isolate (v148R) was amplified and viral RNA was extracted from v148R using the QIAamp viral RNA minikit (Qiagen, Valencia, CA). Viral RNA was reverse transcribed into cDNA using the SuperScript III one-step reverse transcription-PCR (RT-PCR) system with platinum *Taq* (Invitrogen). The entire cDNA genome was sequenced at the Oregon State University Center for Genome Research and Biocomputing Core Laboratories (Corvallis, OR) and analyzed for mutations.

Plaque reduction assay. A plaque reduction assay was performed to compare the level of resistance of v148R and wild-type DENV-2 to that of ST-148. Vero cells were seeded at 3.0×10^5 cells per well in 6-well plates and incubated overnight. Growth medium was aspirated from the plates and cells were infected with DENV-2 or v148R at 100 PFU per well in MEM supplemented with 1% FBS in the presence of 5 μM ST-148 or an equal volume of DMSO. After 1.5 h of incubation, the inoculum was aspirated and the cells were overlaid with a 1:1 mix of SeaPlaque agarose and 2× MEM in the presence of 5 μM ST-148 or an equal volume of DMSO. The plates were incubated for 7 days and fixed and stained as described above with the exception of a shorter stain period (10 s) to visualize plaques.

Multicycle growth curve. A multicycle growth curve was performed to compare the replication fitness of v148R to that of wild-type DENV-2. Vero cells were seeded at 3.0×10^4 cells per well in 12-well plates and incubated overnight. Growth media were aspirated from the plates and cells were infected with DENV-2 or v148R at an MOI of 0.1. After 1.5 h of incubation, the inoculum was removed, replaced with fresh media, and incubated. The supernatant was harvested at various time points and virus levels quantified by plaque assay on Vero cells.

Reverse genetics. DENV-2 cDNA-Tonga/74 and *Escherichia coli* BD1528 *ung*-1 *nadB7* (BD1528) cells were provided by Steve Whitehead at the National Institutes of Health (Bethesda, MD). The S34L mutation identified in v148R was reverse engineered into cDNA and transfected to obtain an infectious virus (vcDNA-148R) to confirm the presence of the resistance-generating mutation. The S34L mutation was generated in DENV-2 cDNA-Tonga/74 using a QuikChange II XL site-directed mutagenesis kit (Agilent Technologies, Santa Clara, CA) and primers DenMut-Cap-S34L-F (5′ TTGACAAAGAGATTCTTACTTGGAATGCTG CAG) and DenMut-Cap-S34L-R (5′ CTGCAGCATTCCAAGTAAGAAT CTCTTTGTCAA) by following the manufacturer's instructions, transformed into competent BD1528 cells, and plated on LB plates containing 10 μg/ml tetracycline. Colonies were picked and cultured, and cDNA was extracted using the QIAquick MiniPrep kit (Qiagen). The cDNA was sequenced to confirm the presence of the mutation of interest. cDNA-S34L was linearized and transcribed with the AmpliCap SP6 high-yield message maker kit (Epicentre, Madison, WI) and purified with an RNeasy minikit (Qiagen). In 6-well plates 24 h prior to infection, Vero cells were seeded at 3.0×10^5 cells per well in MEM with 10% FBS. Five h prior to infection, the medium was removed, washed three times with Dulbecco's phosphate-buffered saline without calcium and magnesium (DPBS) (Cellgro, Manassas, VA), and replaced with Opti-Pro serum-free media (Invitrogen). Transcribed RNA (1 μg) diluted in 20 mM HEPES-saline was added to diluted DOTAP liposomal transfection reagent (Roche, Indianapolis, IN) and HEPES-saline in a polystyrene tube and incubated for 10 min at room temperature. The DOTAP mixture was added to 1 ml of Opti-Pro medium on Vero cells and incubated for 48 h, after which 2 ml of Opti-Pro was added. After 6 days, the transfection was serially diluted on Vero cells as described above, incubated for 7 days, and then fixed and stained as described above to determine the presence of infectious vcDNA-148R viral particles.

C protein purification and expression. The DENV mature capsid domain (positions 1 to 101) was amplified by PCR using cDNA-Tonga/74 (26) as a template and primers DenCap (5′-phosphorylated AATAACCA ACGGAAAAAGGCGAG) and DenCapRevHindIII (5′TCAGTCAAGCT TCATACAGTTCTACGTCTCCTGTTTAAG). The PCR product was digested with StuI and HindIII and cloned into pQE-30Xa vector (Qiagen). The PCR-amplified region was verified by sequencing. Plasmids containing the correct insert were transformed into the *E. coli* M15[pREP4] expression system (Qiagen) according to the manufacturer's protocol. Cultures were incubated at 37°C with shaking until they reached an optical density (OD) of 0.75, were induced with the addition of isopropyl-β-D-thiogalactopyranoside (IPTG) to a final concentration of 1 mM, and were incubated at 37°C for 5 h with shaking. Cultures were harvested by centrifugation at 8,000 × *g* for 20 min, and cell pellets were frozen overnight. Pellets were resuspended in a pH 7.8 binding buffer {20 mM imidazole, 2 mM tris(2-carboxyethyl)phosphine (TCEP), 0.5% 3-[(3-cholamidopropyl)-dimethylammonio]-1-propanesulfonate, 1 M NaCl, and 20 mM HEPES with a complete EDTA-free protease inhibitor cocktail tablet [Roche]}, microfluidized, centrifuged at 20,000 × *g* for 30 min, and filtered. Supernatant was passed through a preequilibrated 5-ml HisTrap HP column (GE Healthcare, Waukesha, WI) and eluted in the same buffer as that described above except containing 500 mM imidazole. Fractions containing histidine-tagged dimerized C protein were frozen at −80°C.

Intrinsic fluorescence. Fluorescence measurements were taken using a Fluorolog-3 fluorescence spectrophotometer (HORIBA Jobin Yvon, Edison, NJ) equipped with a mercury arc lamp. A scan was performed on C protein samples diluted in DPBS using an excitation wavelength of 295 nm and emission wavelengths from 310 to 380 nm in the presence and absence of compound. C protein was diluted until the peak fluorescence

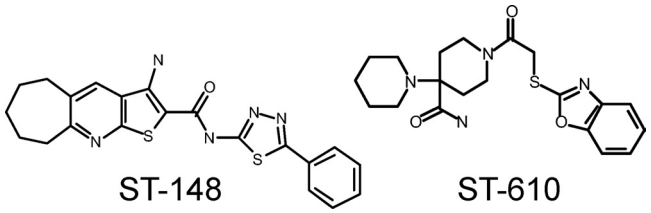

FIG 1 Structures of ST-148 and ST-610.

count measured was between 1 and 2 million counts, which were not saturating for the detection system. Background DPBS and drug fluorescence measurements were also performed, and the signals were subtracted from each sample so that the specific C protein signal was measured in the presence and absence of compound. Samples were prepared in 500-μl volumes for use in a quartz microcuvette. Each experiment was performed in triplicate. Data analysis and collection were performed using DataMax software, version 2.20, installed on a SpectraAcq processor (HORIBA Jobin Yvon).

***In vivo* studies.** All studies involving vertebrate animals were approved by the Institutional Animal Care and Use Committee of Oregon State University, a fully AAALAC-accredited facility, and followed all federal guidelines as outlined in the Guide for the Care and Use of Laboratory Animals (37). Strain 129 (129S2/SvPasCrl) mice were obtained from Charles River Laboratories (Wilmington, DE) and were approximately 6 weeks of age for the pharmacokinetic studies. AG129 mice (alpha/beta interferon [IFN-α/β] and IFN-γ receptor deficient on the strain 129 background) were purchased from B & K Universal (Hull, United Kingdom) and were 5 to 6 weeks of age for antiviral efficacy studies.

Pharmacokinetic analysis. ST-148 was formulated for oral (per os [p.o.]), intraperitoneal (i.p.), and intravenous (i.v.) dosing of mice (strain 129) as an aqueous solution in 32% hydroxypropyl-beta-cyclodextrin (HPβCD) (Roquette, Lestrem, France). ST-148 concentrations were measured in plasma harvested from mice at approximately 0.08, 0.25, 0.5, 1, 2, 3, 4, 6, 8, and 24 h after i.v. administration and 1, 2, 3, 4, 6, 8, and 24 h after p.o. and i.p. administration. Compound concentrations were measured by liquid chromatography-tandem mass spectrometry (LC-MS/MS) using a 3200 Q Trap LC-MS/MS system (Applied Biosystems/MDS Sciex, Foster City, CA). LC was performed with a Phenomenex Synergi JAX-RP column (4-μm particle size; 50 mm by 2 mm) at a flow rate of 0.5 ml/min with a mobile phase containing 20% acetonitrile, 80% 10 mM ammonium formate, pH 3.5, in water. WinNonlin software (Pharsight, Sunnyvale, CA) was used to estimate pharmacokinetic values.

Antiviral efficacy in dengue murine model. DENV-2 strain NGC was used in the mouse model and was propagated in C6/36 mosquito cells. Five- to 6-week-old female AG129 mice were housed appropriately in labeled cages (4 mice per cage), identified by ear notching, and weighed prior to any other procedures. Mice were injected i.p. with 0.5 ml of virus suspension in PBS (1.3×10^6 PFU per mouse). Mice were dosed immediately postchallenge with either 50 mg/kg of body weight of ST-148 or the same volume of vehicle. Weight measurements and clinical observations were made daily. On day 3 postinfection, mice were sacrificed by CO_2 asphyxiation. Spleen and liver samples were taken from each animal and transferred to preweighed homogenization tubes (FastPrep-24 Lysing Matrix C with an additional 1/4-inch ceramic sphere added; MP Biomedical, Solon, OH) with 0.5 ml of DPBS. Blood was collected into Eppendorf tubes containing sodium citrate for plasma isolation. Plasma viremia and tissue viral load were determined by plaque titration. Plasma cytokine (interleukin-6 [IL-6], IL-10, IL-12p70, IFN-γ, tumor necrosis factor alpha [TNF-α], and monocyte chemoattractant protein 1 [MCP-1]) levels were assessed using the BD cytometric beat array (CBA) mouse inflammation kit per the manufacturer's instructions (BD Biosciences, San Jose, CA).

Statistical analysis. For comparison of viral load in the plasma, spleen, and liver as well as cytokine levels in the plasma among vehicle groups and groups treated once daily (QD) and twice daily (BID) with ST-148, one-way analysis of variance (ANOVA) with a Holm-Sidak correction was used. For comparison of these parameters between vehicle-treated groups and groups treated with ST-148 three times a day (TID), an unpaired Student *t* test was used; $P < 0.05$ was considered statistically significant. SigmaPlot for Windows version 11.0 was used for performing all statistical analyses (Systat Software, Inc., San Jose, CA).

TABLE 1 Antiviral activity of ST-148 against DENV

Cell type	Virus	EC_{50}[a] (μM)
Vero	DENV-1	2.832 ± 1.13
	DENV-2	0.016 ± 0.01
	DENV-3	0.512 ± 0.42
	DENV-4	1.150 ± 0.14
	DENV-2 K0049	0.551 ± 0.40
	DENV-2 S221	0.023 ± 0.01
	v148R	8.918 ± 0.80
	vcDNA-148R	8.684 ± 0.75
C6/36	DENV-2	0.039 ± 0.01
Huh-7	DENV-2	0.012 ± 0.01
BHK	DENV-2	0.073 ± 0.08
L929	DENV-2	0.016 ± 0.01

[a] Cells were infected with the indicated viruses at an MOI of 0.1 and treated with ST-148. Culture medium was collected at 48 h postinfection, and the viral titer was determined by plaque assay. For K0049, activity was measured by ELISA. v148R is the tissue culture-passaged, drug-resistant DENV-2 isolate, and vcDNA-148R is the virus recovered from the engineered cDNA clone. The data are mean values ± SD from three independent experiments.

RESULTS

ST-148 is a potent inhibitor of DENV replication *in vitro*. ST-148 (Fig. 1) was identified through a high-throughput screening (HTS) assay of approximately 200,000 chemically diverse compounds. The HTS assay was developed to identify inhibitors of DENV replication as measured by inhibition of virus-induced CPE in a 96-well plate format. ST-148 inhibited DENV-2 in a viral titer reduction assay with an EC_{50} (the concentration of compound necessary to inhibit 50% of the virus titer) of 0.016 μM (Table 1) and an EC_{90} of 0.125 μM. While ST-148 was active against other dengue serotypes, the compound exhibited a broad range of potencies, with EC_{50}s of 0.512, 1.150, and 2.832 for DENV-3, -4, and -1, respectively. Analogs of ST-148 with improved potency were more active against all four serotypes and the range of EC_{50}s was more narrow, suggesting that these analogs

TABLE 2 Cell toxicity of ST-148

Cell type	CC_{50}[a] (μM)
Vero (2 days)	>100
Vero (5 days)	>100
BSC40	>100
C6/36	>100
Huh-7	>100
BHK	>100
MDBK	>100
L929	>50

[a] Cells were incubated with ST-148 at a range of concentrations for 48 h (also 5 days for Vero cells and 96 h for MDBK cells). Cell viability was measured using a resazurin assay where the absorbance was measured on an EnVision multilabel reader at 5 h after the addition of resazurin and incubation at 37°C. For the 5-day assay, viability was measured using the Cell Titer-Glo luminescent cell viability assay. The data are mean values from three independent experiments.

TABLE 3 ST-148 antiviral spectrum of activity and selectivity

Virus	Family	Genus	Group[c]	EC_{50} (μM)
Modoc virus	*Flaviviridae*	*Flavivirus*	+ssRNA	0.36
Yellow fever virus[a]	*Flaviviridae*	*Flavivirus*	+ssRNA	6.97
Japanese encephalitis virus[a]	*Flaviviridae*	*Flavivirus*	+ssRNA	>50
Bovine viral diarrhea virus	*Flaviviridae*	*Pestivirus*	+ssRNA	>50
Hepatitis C virus[b]	*Flaviviridae*	*Hepacivirus*	+ssRNA	39.2
Sindbis virus	*Togaviridae*	*Alphavirus*	+ssRNA	>50
Influenza A virus	*Orthomyxoviridae*	*InfluenzavirusA*	−ssRNA	>25
Vaccinia virus	*Poxviridae*	*Orthopoxvirus*	dsDNA	>50
Herpes simplex virus 1	*Herpesviridae*	*Simplexvirus*	dsDNA	>50

[a] *In vitro* testing done by Integrated Biotherapeutics via a CPE-based assay in Vero cells.
[b] *In vitro* testing done by the Neyts laboratory at the Rega Institute using a subgenomic HCV replicon (genotype 1b) in Huh 5.2 cells (27).
[c] ssRNA, single-stranded RNA; dsDNA, double-stranded DNA; +, plus strand; −, minus strand.

were better optimized to interact with the viral target. ST-148 had potent activity against all four serotypes of DENV in various cells types, including Vero, C6/36, Huh-7, BHK, and L929 cells. ST-148 was not cytotoxic in any of the cell lines tested (Table 2).

ST-148 selectively inhibits flaviviruses. To determine the spectrum of antiviral activity, ST-148 potency was measured against a variety of viruses from different virus families. As shown in Table 1 and Table 3, ST-148 was active against all DENV serotypes and Modoc virus, a murine flavivirus, but showed less activity against other members of the *Flaviviridae* family and did not effectively inhibit viruses outside the *Flaviviridae* family. These results indicated that ST-148 selectively inhibits DENV within the *Flavivirus* genus.

ST-148 is not mutagenic. To evaluate the mutagenic potential of ST-148, the compound was tested in the bacterial reverse mutation assay and the Muta-Chromo plate assay using *Salmonella* Typhimurium tester strains TA-98, TA-100, TA-1535, and TA-1537 as well as *Escherichia coli* tester strain WP-2 *uvrA* in the presence and absence of Aroclor-induced rat liver S9. No mutagenic potential was observed with any of these conditions.

Time-of-drug-addition studies. To investigate which stage of the viral life cycle is affected by ST-148, a time-of-drug-addition experiment was conducted where 25 μM ST-148 was added to DENV-2-infected Vero cells either just before the time of infection or at several time points after infection. At 48 h postinfection, viral yield was quantified by plaque assay. The data indicate that ST-148 inhibits virus replication up to 12 h after infection, which is consistent with a postentry mechanism of action (Fig. 2A).

Isolation of drug-resistant virus variants. To identify determinants of ST-148 sensitivity, virus variants resistant to the inhibitory effects of the compound were generated by 10 serial passages of virus in the presence of ST-148. Virus capable of growing in the presence of 5 μM ST-148 (corresponding to a 312-fold higher EC_{50}) was isolated and plaque purified three times in the presence of compound. A plaque reduction assay was conducted to mea-

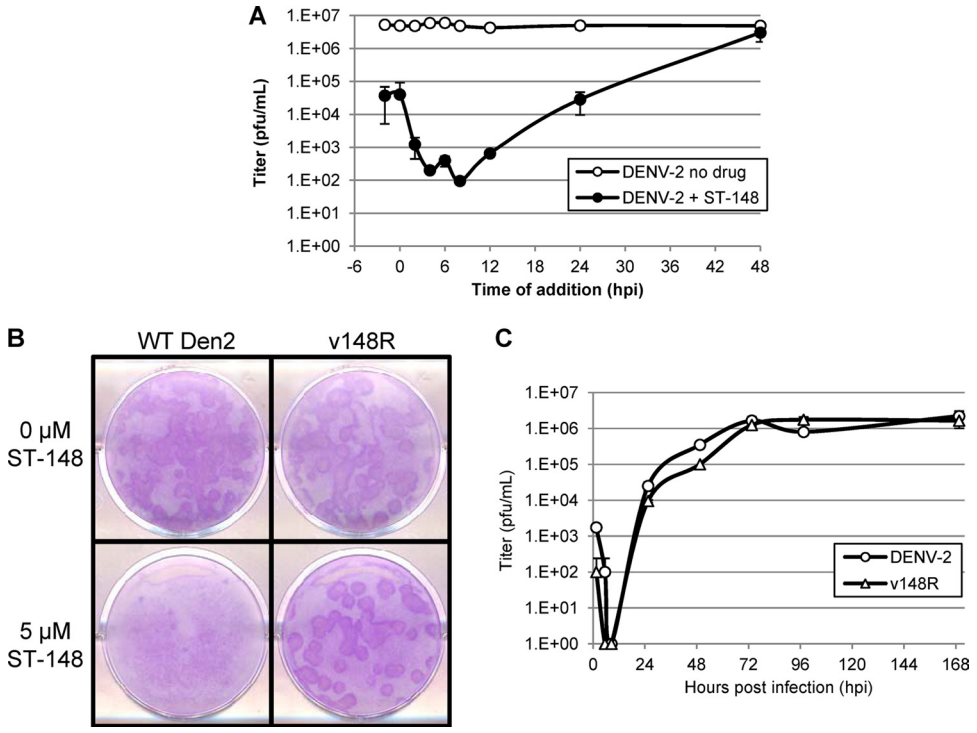

FIG 2 (A) Time-of-drug-addition study. DENV-2-infected Vero cells were treated with 25 μM ST-148 at various time points, and virus levels were quantified by plaque assay at 48 hpi. The data are mean values ± standard deviations (SD) from three independent experiments. (B) Plaque formation of wild-type DENV and ST-148-resistant virus in the presence and absence of ST-148. Vero cell monolayers were infected with DENV-2 or v148R in the presence and absence of 5 μM ST-148 and covered with an agarose overlay. At 7 days postinfection the cultures were fixed in 5% glutaraldehyde and stained with crystal violet. (C) Multicycle growth curve of wild-type DENV and ST-148-resistant virus in the absence of ST-148. Vero cell monolayers were infected with virus and harvested at various time points, and plaques were titrated. The data are mean values ± SD from two observations.

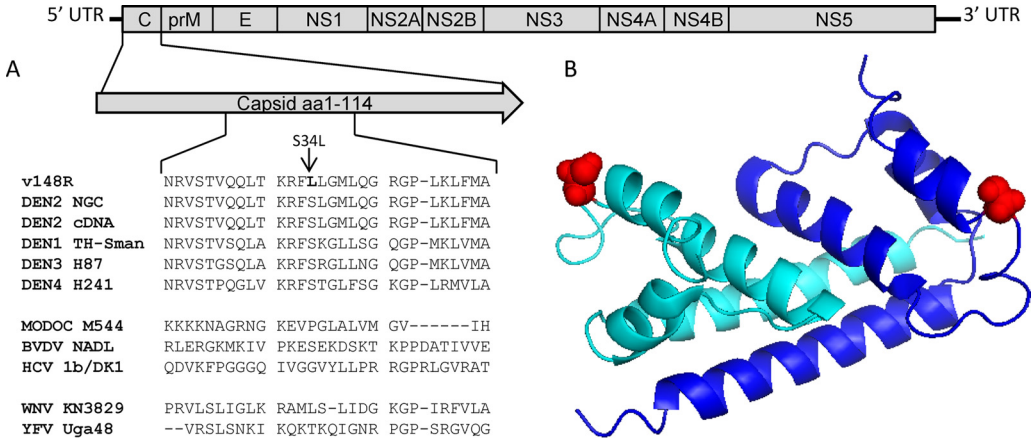

FIG 3 (A) Sequence comparison of capsid orthologs. Shown is a graphic representation of the DENV genome, illustrating the location of resistance to ST-148 (capsid S34L), and an amino acid sequence comparison of orthologs from the capsid region of other flaviviruses showing the degree of sequence conservation. (B) Structure of the homodimer DENV-2 C protein. Subunit A, light blue; subunit B, dark blue. The location of the serine residue at position 34 is indicated in red for both chains. The protein structure was modified using CN3D software (33).

sure the ST-148 sensitivity of this variant (designated v148R) relative to wild-type virus. In the presence of ST-148, plaque formation of the wild-type virus was greatly reduced, both in size and number, while equal numbers of plaques, similar in size to those of the non-drug-treated samples, were observed for v148R in the presence of compound (Fig. 2B). The plaques are visualized by crystal violet staining with the stain in contact with the monolayer for a very short duration (just a few seconds). The cytopathic effects resulting from dengue virus replication appear to enhance dye binding relative to that in the uninfected monolayer, resulting in plaques binding more dye and staining darker. This rapid staining technique is used to visualize plaques formed by many types of virus that fail to form obvious plaques on cell monolayers. In multicycle growth experiments the replication rate and peak titer of v148R in the absence of compound was similar to that of wild-type virus, suggesting that mutations affecting drug susceptibility had no measurable effect on viral fitness (Fig. 2C), at least *in vitro*. A viral titer reduction assay was used to determine the level of susceptibility of the resistant virus to ST-148. The EC_{50} for inhibition of the resistant variant (8.92 μM) was more than 550-fold higher than the EC_{50} for inhibition of wild-type DENV-2 as determined in Vero cells (0.016 μM) (Table 1).

ST-148 resistance maps to the capsid coding region. Genomic RNA from plaque-purified resistant virus was isolated and amplified by reverse transcription-PCR to generate cDNA. The nucleotide sequence of overlapping segments of the cDNA from the resistant variant was determined and compared to the wild-type DENV sequence to identify the changes in the viral genome that correlated with reduced compound susceptibility. A single-nucleotide change (nucleotide 101 in the capsid gene, cytosine to thymine) was found in the resistant virus genome that resulted in a predicted change of serine (Ser) to leucine (Leu) at amino acid position 34 in the capsid gene (Fig. 3). Each of the DENV serotypes, but not Modoc virus, has a serine at position 34. This change was reengineered into wild-type DENV-2 cDNA in order to confirm that the single mutation found was responsible for conferring resistance to ST-148. Infectious virus recovered from the engineered cDNA clone (vcDNA-148R) showed reduced susceptibility to ST-148 with an EC_{50} for inhibition of 8.68 μM, similar to the parental resistant isolate (Table 1). These results support the conclusion that the S34L mutation is sufficient to confer resistance to ST-148.

ST-148 interacts with C protein. Compounds that bind proteins can alter the dielectric properties of aromatic amino acid residues, causing a change in the intrinsic fluorescence of the protein. To determine if ST-148 interacts with C protein, its intrinsic fluorescence was measured from 310 to 380 nm in the presence and absence of ST-148. In the presence of ST-148, a dose-dependent decrease in the intrinsic fluorescence was observed, which is consistent with a direct interaction of the compound with C protein (Fig. 4A). As controls, the intrinsic protein fluorescence was measured in the presence of DMSO only or in the presence of ST-610, a DENV inhibitor compound discovered at SIGA that has a different chemical structure and targets the helicase enzyme (unpublished data) (Fig. 1 and 4C). Neither DMSO nor ST-610 had a substantial effect on the intrinsic protein fluorescence, suggesting that the effects on fluorescence induced by ST-148 were specific. Similar results were observed with a C protein variant isolated from ST-148-resistant virus (Fig. 4B and D). These results suggest that ST-148 interacts with C protein but that amino acid changes that correlate with reduced compound susceptibility do not alter this interaction.

Pharmacokinetic analyses and tolerability. The pharmacokinetic parameters of ST-148 in mice were determined after formulating the compound as an aqueous solution in 32% hydroxypropyl-beta-cyclodextrin (HPβCD). Oral or intraperitoneal administration of ST-148 at 50 mg/kg/day in strain 129 mice generated peak plasma concentrations of 3,138 or 52,283 ng/ml (7.44 or 124.04 μM), respectively (Table 4), which are 468- and 7,750-fold above the *in vitro* EC_{50}. Intravenous administration of ST-148 at 20 mg/kg/day generated a peak plasma concentration of 41,133 ng/ml (97.58 μM), 6,093-fold above the EC_{50}. The area under the plasma concentration-time curve (AUC) was greatest in mice administered ST-148 via the i.p. route. The absolute oral bioavailability of ST-148 was 9.1%. The compound was rapidly absorbed after oral dosing, and the time to maximum plasma concentration was measured at 1.0 h. Intraperitoneal administration produced higher plasma con-

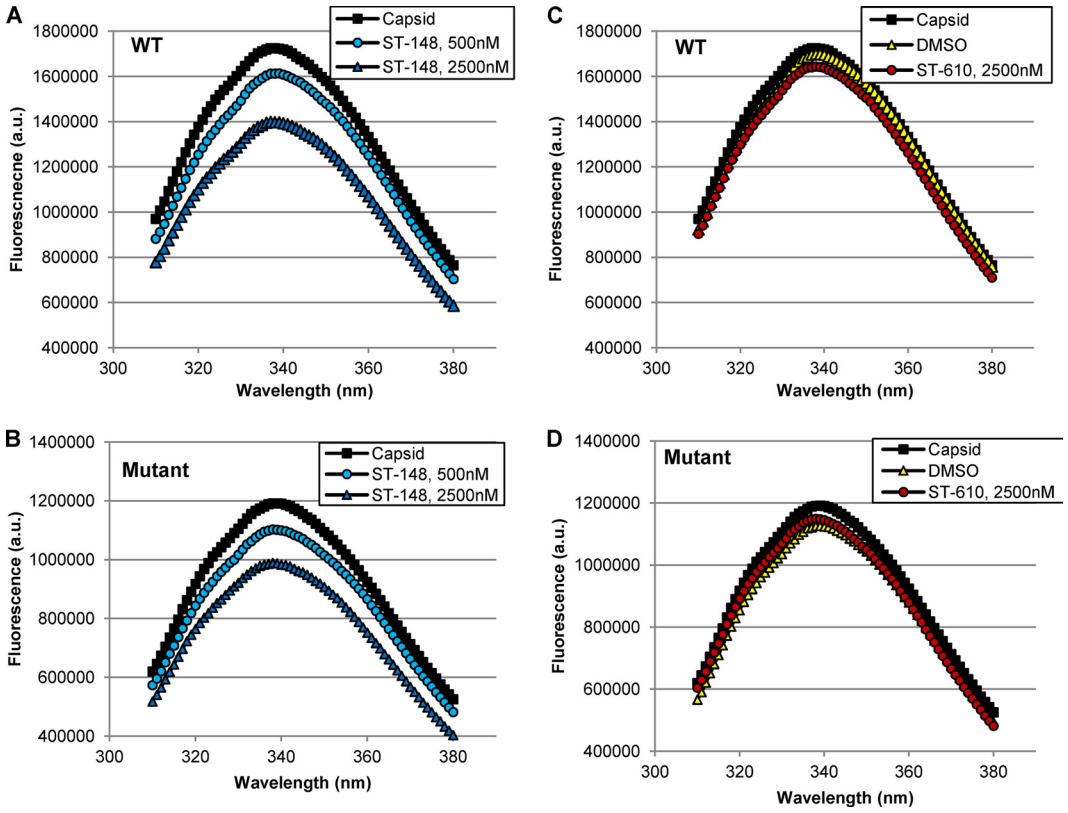

FIG 4 Effect of ST-148 on the intrinsic fluorescence of C protein. Intrinsic fluorescence measurements in arbitrary units (a.u.) were made by combining protein and compound and reading the absorbance at an excitation of 295 nm and scanning emissions between 310 and 380 nm. (A) C protein in the presence of ST-148, (B) ST-148-resistant mutant C protein (S34L) with ST-148, (C) C protein with ST-610, and (D) mutant C protein with ST-610.

centrations with rapid absorption and peak plasma drug concentrations at 1.0 h after dosing. There was no overt toxicity or changes in physical signs, including body weights, observed in mice after repeated oral or i.p. ST-148 administration of 50 mg/kg/day for 3 days. These data indicate that ST-148 has limited oral bioavailability and fairly rapid clearance but good systemic availability following i.p. administration.

***In vivo* antiviral efficacy.** A murine viremia model (28–30) using AG129 mice, which are deficient for IFN-α/β and -γ receptors, was used to evaluate the *in vivo* efficacy of ST-148. Infection of AG129 mice with DENV-2 (strain NGC) via intraperitoneal inoculation with 1.3×10^6 PFU produces a nonlethal infection with peak of viremia occurring on day 3 postinfection and an elevation in cytokine levels that is characteristic of DF. Immediately after infection, ST-148 or vehicle at 50 mg/kg/dose was administered either once (QD) or twice (BID) daily for 3 days. There were no additional weight changes in the ST-148-treated mice compared to vehicle-treated mice during the course of the experiment. On average, BID treatment with ST-148 reduced peak plasma viremia 52-fold and reduced viral load in the spleen and liver 3- and 20-fold, respectively (Fig. 5A). This difference in viremia relative to vehicle-treated mice was statistically significant as determined by one-way ANOVA (Table 5). An increase in the level of inflammatory cytokines has been observed in the blood of patients who have DF (31) and has a contributing role in vascular leakage and disease severity. In the AG129 model, levels of TNF-α, IL-6, MCP-1, and IFN-γ are elevated, and a trend toward lower levels was observed in mice receiving ST-148 BID (Fig. 5B and C), which was not statistically significant.

We further tested whether ST-148 was active in this model when administered orally. Due to ST-148 p.o. pharmacokinetics that result in plasma levels of ST-148 above the *in vitro* EC_{90} for only approximately 8 h after administration, the compound was administered three times per day (TID) at 8-h intervals at 50 mg/kg/dose for three consecutive days. On average, treatment with ST-148 TID reduced peak viremia 3-fold and reduced viral load in the spleen and liver 7- and 9-fold, respectively (Fig. 6A). This difference in viremia relative to vehicle-treated mice was statistically significant as determined by one-way ANOVA (Table 6). ST-148 administered orally showed a trend toward reduced levels of TNF-α, MCP-1, and IL-6 but not IFN-γ, but the levels were not statistically significant (Fig. 6B and C).

Taken together, these results illustrate that ST-148 can decrease viremia, viral load in tissues, and inflammatory cytokine levels when administered either i.p. or orally.

TABLE 4 Pharmacokinetic parameters of ST-148 in strain 129 mice[a]

Route	Dose (mg/kg)	T_{max} (h)	C_{max} (ng/ml)	AUC (h · ng/ml)
p.o.	50	1.0	3,138	5826
i.p.	50	1.0	52,283	77,011
i.v.	20	0.1	41,133	25,523

[a] Plasma drug concentrations were measured by LC-MS/MS over a 24-h time period. T_{max}, time of maximal concentration; C_{max}, maximal concentration.

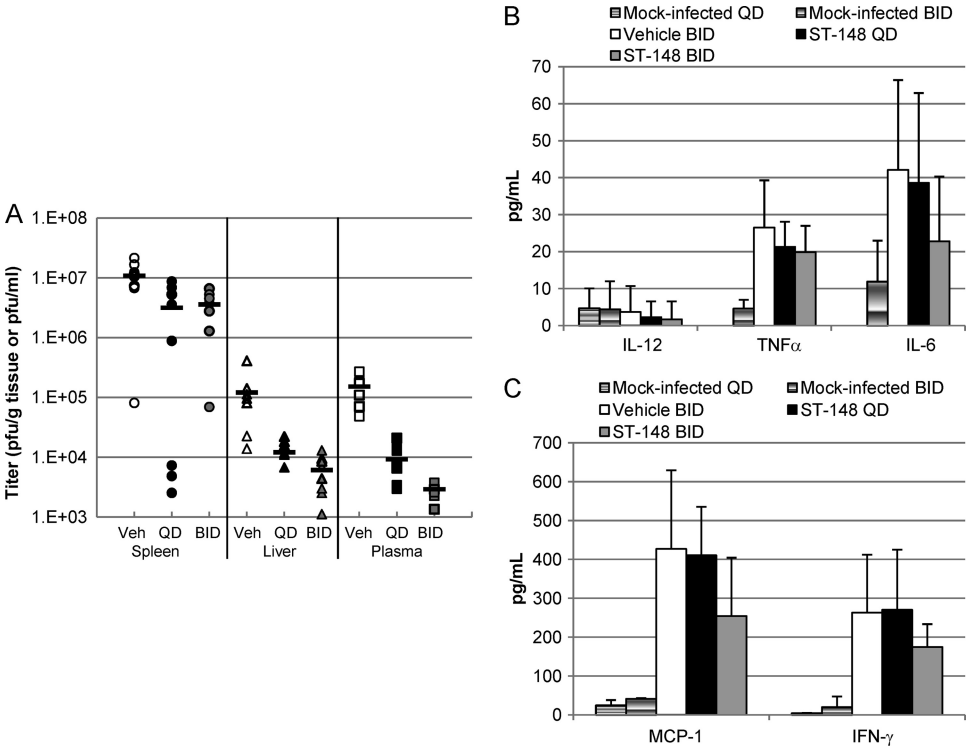

FIG 5 *In vivo* efficacy of ST-148 delivered i.p. AG129 mice (8 mice/treatment group) were infected with 1.3×10^6 PFU DENV-2 (strain NGC) i.p. on day 0. The mice were treated with 50 mg/kg ST-148 i.p. either once (QD) or twice per day (BID). On day 3 postinfection (the peak of viremia), the viral load and viremia were quantified by plaque assay. (A) Viral load and viremia. White symbols represent vehicle-treated mice (Veh), black symbols represent mice treated with ST-148 QD, and gray symbols represent mice treated with ST-148 BID. Circles represent spleen titer, triangles represent liver titer, and squares represent plasma titer. Solid bars represent the arithmetic means. (B and C) Inflammatory cytokine levels in the plasma. The lower limit of quantification for the CBA assay is 20 pg/ml. The data are mean values ± SD from three observations.

DISCUSSION

A high-throughput screen was conducted to identify inhibitors of DENV-induced cytopathic effects. Characterization of compounds from this screen identified a chemical series that inhibited the replication of all four DENV serotypes. The lead compound in this series, ST-148, exhibited strong DENV-2 antiviral activity with an EC_{50} of 16 nM and a CC_{50} (concentration of compound causing a 50% reduction in cell viability as a percentage of untreated cells) of >50 μM in several transformed cell types. ST-148 was inactive against Japanese encephalitis virus and BVDV but showed substantial activity against Modoc virus (EC_{50} = 0.36 μM) and weak activity against yellow fever virus (EC_{50} = 6.97 μM) and hepatitis c virus (HCV) (EC_{50} = 39.2 μM). The weak activity against HCV was likely nonspecific, since this assay was conducted using a subgenomic replicon system that lacks C protein. ST-148 was not active against representative viruses from other virus families. The compound was not genotoxic in Ames tests and was well tolerated in mice but exhibited modest oral bioavailability (9.1%). Administration of ST-148 to mice lacking interferon receptors, via either oral gavage or intraperitoneal injection at 50 mg/kg, reduced the viremia and viral load in the liver and spleen by 1 log, suggesting that the compound is active *in vivo*.

TABLE 5 Viral titer from mice treated with ST-148 i.p. at 50 mg/kg/dose

Treatment and organ	Mean titer (PFU/g tissue or PFU/ml)	SD	*P* value vs vehicle
Vehicle			
Spleen	1.08×10^7	6.48×10^6	
Liver	1.21×10^5	1.23×10^5	
Plasma	1.52×10^5	7.19×10^4	
ST-148 QD			
Spleen	3.16×10^6	3.47×10^6	0.002
Liver	1.21×10^4	6.83×10^3	0.004
Plasma	9.20×10^3	6.81×10^3	<0.001
ST-148 BID			
Spleen	3.59×10^6	2.14×10^6	0.004
Liver	6.12×10^3	4.06×10^3	0.006
Plasma	2.93×10^3	8.33×10^2	<0.001

DENV variants with reduced susceptibility to ST-148 were isolated and compound susceptibility determinants mapped to the region of the genome encoding the C protein. An amino acid substitution from serine to leucine at position 34 of the C protein correlated with a loss of compound susceptibility. These results suggest that ST-148 interacts with the C protein to inhibit DENV replication.

A direct interaction of ST-148 with the C protein was measured by compound-induced effects on the intrinsic protein fluorescence. The reduction in intrinsic fluorescence of C protein in the presence of ST-148 was not observed in the presence of an unrelated compound, ST-610, that also inhibits DENV replication but targets the helicase protein. While these data suggest a specific

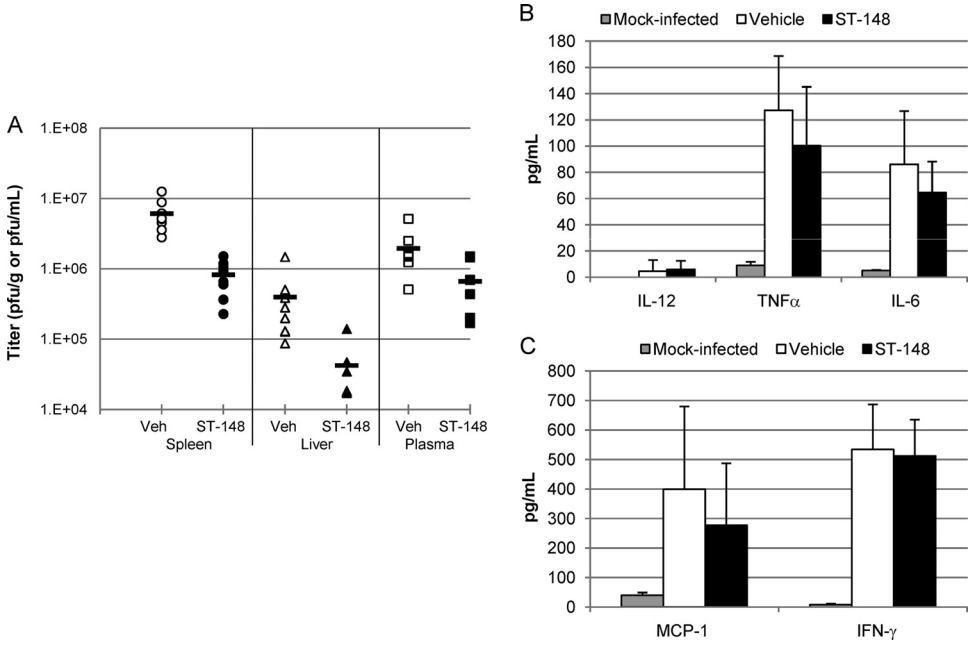

FIG 6 Oral *in vivo* efficacy of ST-148. AG129 mice (8 mice/treatment group) were infected with 9×10^6 PFU DENV-2 (strain NGC) i.p. on day 0. The mice were treated with 50 mg/kg ST-148 p.o. three times per day (TID). On day 3 postinfection (the peak of viremia), the viral load and viremia were quantified by plaque assay. (A) For viral load and viremia, open symbols represent vehicle-treated mice and filled symbols represent ST-148-treated mice. Circles represent spleen titer, triangles represent liver titer, and squares represent plasma titer. Solid bars represent the arithmetic means. (B and C) Inflammatory cytokine levels in plasma. The lower limit of quantification for the CBA assay is 20 pg/ml. The data are mean values ± SD from three observations.

interaction of ST-148 with the C protein, similar results were observed using a mutant C protein that contained the S34L change associated with reduced compound susceptibility. Furthermore, ST-148 showed substantial antiviral activity against Modoc virus, a natural flavivirus pathogen of mice, and yellow fever virus. A comparison of the amino acid residues of DENV C protein to those of selected flaviviruses, including Modoc virus and yellow fever virus, did not provide an obvious explanation as to why these viruses would be susceptible to ST-148 while other flaviviruses were not. It is possible that the interaction of ST-148 with the mutant C protein induces a conformational change that blocks the normal function of the C protein but not its intrinsic fluorescence properties. It is also possible that ST-148 interacts with another region of the protein to affect intrinsic protein fluorescence and the S34L amino acid change prevents inhibition by ST-148 without blocking this interaction. Taken together, these data suggest that ST-148 interacts with the C protein and blocks an essential activity required for virus replication.

TABLE 6 Viral titer from mice treated with ST-148 p.o. at 50 mg/kg/dose

Organ	Mean titer (PFU/g tissue or PFU/ml)	SD	*P* value vs vehicle
Vehicle			
Spleen	6.08×10^6	3.16×10^6	
Liver	3.98×10^5	4.56×10^5	
Plasma	1.95×10^6	1.39×10^6	
ST-148 TID			
Spleen	8.20×10^5	4.35×10^5	<0.001
Liver	4.22×10^4	4.11×10^4	0.046
Plasma	6.65×10^5	5.44×10^5	0.029

Time-of-drug-addition experiments suggest that ST-148 is maximally effective when added before or at the time of infection (Fig. 2A), which suggests inhibition of uncoating, which is consistent with an earlier report on the entry kinetics of DENV (32). Given that the level of DENV released from infected cells is still somewhat reduced when ST-148 is added up to 24 h after infection, it is also possible that ST-148 interaction with the C protein has an additional effect on later stages of viral morphogenesis, such as nucleocapsid assembly. Alternatively, the assay may be measuring virus spread, as an inhibition event at an early stage may be amplified because of multiple rounds of virus infection and spread. However, as it is likely the C protein has multiple functions in uncoating, replication, and assembly of progeny virions, more work is needed to understand the overall effect of ST-148.

The mature form of the C protein is a basic, 12-kDa protein that forms homodimers in solution consisting of four alpha helices (α1 to α4). They are arranged in the dimer to produce a concave-shaped molecule (33). The floor of the C protein dimer is composed of the highly basic α4-α4′ helices, which are thought to interact with RNA. At the top of the concave structure, α2-α2′ and α1-α1′ helices have been proposed to interact with membranes (33). Based upon this structure, it has been proposed that positively charged residues on α1-α1′ helices are involved in membrane interactions (33). The amino acid change (S34L) associated with compound susceptibility resides at the end of the α1-α1′ helices (Fig. 3B). Perhaps ST-148 interacts with this region of the protein and prevents membrane association or other essential functions required for viral replication. Although the C protein is the least conserved of the flavivirus pro-

teins, the structural properties are very similar and the charge distribution is well conserved.

The C protein binds RNA, which is consistent with a proposed role in encapsidation of newly replicated RNA into virions. A fraction of the cytoplasmic C protein in DENV-infected cells accumulates on the surface of ER-derived organelles named lipid droplets (34). A similar phenotype was observed in cell lines expressing HCV C protein (35). Substitutions of amino acid L50 or L54 in the DENV C protein disrupted lipid droplet targeting and impaired viral particle formation. Likewise, mutations that disrupt lipid droplet association of HCV C protein reduced particle formation (36). Moreover, one study proposed that DENV infection increased the number of lipid droplets per cell (34). Taken together, these results suggest that there is a link between lipid droplet metabolism and viral replication (34). It is possible that ST-148 alters the interaction between lipid droplets and the C protein, thereby inhibiting viral replication. While the S34L change did not appear to alter interaction between C protein and ST-148 based upon the results of the intrinsic protein fluorescence experiments, this amino acid change could bypass the inhibitory effects of the compound by facilitating membrane association. Further studies are ongoing to elucidate the mechanism of ST-148 inhibition.

ACKNOWLEDGMENTS

This work was supported by NIH grants 1R43AI079937-01A1 and 1 R01A1093356-01. R. Bartenschlager is supported by grants from the European Union (Silver [grant no. 260644] and Euvirna [grant no. 264286]). This work was performed by employees of SIGA Technologies, incorporated, who hold stock in the company.

We thank Steve Whitehead for the cDNA, Sujan Shresta for the S221 virus, Rebecca Rico-Hesse for the K0049 virus, and Johan Neyts for HCV specificity testing. We also thank Kady Honeychurch for DENV-specific primer design, Andrew Wieczorek and Thuan Tran for HTS support, Candace Lovejoy for project management, and Yali Chen for carrying out the Ames assay. Thanks to Sean Amberg for critical review of the manuscript.

REFERENCES

1. **Deen JL, Harris E, Wills B, Balmaseda A, Hammond SN, Rocha C, Dung NM, Hung NT, Hien TT, Farrar JJ.** 2006. The WHO dengue classification and case definitions: time for a reassessment. Lancet **368**:170–173.
2. **Halstead SB.** 2007. Dengue. Lancet **370**:1644–1652.
3. **Gubler DJ.** 2002. Epidemic dengue/dengue hemorrhagic fever as a public health, social and economic problem in the 21st century. Trends Microbiol. **10**:100–103.
4. **Monath TP.** 1994. Dengue: the risk to developed and developing countries. Proc. Natl. Acad. Sci. U. S. A. **91**:2395–2400.
5. **Dejnirattisai W, Jumnainsong A, Onsirisakul N, Fitton P, Vasanawathana S, Limpitikul W, Puttikhunt C, Edwards C, Duangchinda T, Supasa S, Chawansuntati K, Malasit P, Mongkolsapaya J, Screaton G.** 2010. Cross-reacting antibodies enhance dengue virus infection in humans. Science **328**:745–748.
6. **Vaughn DW, Green S, Kalayanarooj S, Innis BL, Nimmannitya S, Suntayakorn S, Endy TP, Raengsakulrach B, Rothman AL, Ennis FA, Nisalak A.** 2000. Dengue viremia titer, antibody response pattern, and virus serotype correlate with disease severity. J. Infect. Dis. **181**:2–9.
7. **Welsch S, Miller S, Romero-Brey I, Merz A, Bleck CK, Walther P, Fuller SD, Antony C, Krijnse-Locker J, Bartenschlager R.** 2009. Composition and three-dimensional architecture of the dengue virus replication and assembly sites. Cell Host Microbe **5**:365–375.
8. **Cleaves GR, Ryan TE, Schlesinger RW.** 1981. Identification and characterization of type 2 dengue virus replicative intermediate and replicative form RNAs. Virology **111**:73–83.
9. **Zhang Y, Kaufmann B, Chipman PR, Kuhn RJ, Rossmann MG.** 2007. Structure of immature West Nile virus. J. Virol. **81**:6141–6145.
10. **Yu IM, Zhang W, Holdaway HA, Li L, Kostyuchenko VA, Chipman PR, Kuhn RJ, Rossmann MG, Chen J.** 2008. Structure of the immature dengue virus at low pH primes proteolytic maturation. Science **319**:1834–1837.
11. **Zhang Y, Corver J, Chipman PR, Zhang W, Pletnev SV, Sedlak D, Baker TS, Strauss JH, Kuhn RJ, Rossmann MG.** 2003. Structures of immature flavivirus particles. EMBO J. **22**:2604–2613.
12. **Noble CG, Chen YL, Dong H, Gu F, Lim SP, Schul W, Wang QY, Shi PY.** 2010. Strategies for development of Dengue virus inhibitors. Antiviral Res. **85**:450–462.
13. **Poh MK, Yip A, Zhang S, Priestle JP, Ma NL, Smit JM, Wilschut J, Shi PY, Wenk MR, Schul W.** 2009. A small molecule fusion inhibitor of dengue virus. Antiviral Res. **84**:260–266.
14. **Lim SP, Sonntag LS, Noble C, Nilar SH, Ng RH, Zou G, Monaghan P, Chung KY, Dong H, Liu B, Bodenreider C, Lee G, Ding M, Chan WL, Wang G, Jian YL, Chao AT, Lescar J, Yin Z, Vedananda TR, Keller TH, Shi PY.** 2011. Small molecule inhibitors that selectively block dengue virus methyltransferase. J. Biol. Chem. **286**:6233–6240.
15. **Steuer C, Gege C, Fischl W, Heinonen KH, Bartenschlager R, Klein CD.** 2011. Synthesis and biological evaluation of alpha-ketoamides as inhibitors of the Dengue virus protease with antiviral activity in cell-culture. Bioorg. Med. Chem. **19**:4067–4074.
16. **Xie X, Wang QY, Xu HY, Qing M, Kramer L, Yuan Z, Shi PY.** 2011. Inhibition of dengue virus by targeting viral NS4B protein. J. Virol. **85**:11183–11195.
17. **Chen YL, Yin Z, Duraiswamy J, Schul W, Lim CC, Liu B, Xu HY, Qing M, Yip A, Wang G, Chan WL, Tan HP, Lo M, Liung S, Kondreddi RR, Rao R, Gu H, He H, Keller TH, Shi PY.** 2010. Inhibition of dengue virus RNA synthesis by an adenosine nucleoside. Antimicrob. Agents Chemother. **54**:2932–2939.
18. **Niyomrattanakit P, Chen YL, Dong H, Yin Z, Qing M, Glickman JF, Lin K, Mueller D, Voshol H, Lim JY, Nilar S, Keller TH, Shi PY.** 2010. Inhibition of dengue virus polymerase by blocking of the RNA tunnel. J. Virol. **84**:5678–5686.
19. **Wang QY, Kondreddi RR, Xie X, Rao R, Nilar S, Xu HY, Qing M, Chang D, Dong H, Yokokawa F, Lakshminarayana SB, Goh A, Schul W, Kramer L, Keller TH, Shi PY.** 2011. A translation inhibitor that suppresses dengue virus in vitro and in vivo. Antimicrob. Agents Chemother. **55**:4072–4080.
20. **Chang J, Schul W, Butters TD, Yip A, Liu B, Goh A, Lakshminarayana SB, Alonzi D, Reinkensmeier G, Pan X, Qu X, Weidner JM, Wang L, Yu W, Borune N, Kinch MA, Rayahin JE, Moriarty R, Xu X, Shi PY, Guo JT, Block TM.** 2011. Combination of alpha-glucosidase inhibitor and ribavirin for the treatment of dengue virus infection in vitro and in vivo. Antiviral Res. **89**:26–34.
21. **Chang J, Schul W, Yip A, Xu X, Guo JT, Block TM.** 2011. Competitive inhibitor of cellular alpha-glucosidases protects mice from lethal dengue virus infection. Antiviral Res. **92**:369–371.
22. **Courageot MP, Frenkiel MP, Dos Santos CD, Deubel V, Despres P.** 2000. Alpha-glucosidase inhibitors reduce dengue virus production by affecting the initial steps of virion morphogenesis in the endoplasmic reticulum. J. Virol. **74**:564–572.
23. **Whitby K, Pierson TC, Geiss B, Lane K, Engle M, Zhou Y, Doms RW, Diamond MS.** 2005. Castanospermine, a potent inhibitor of dengue virus infection in vitro and in vivo. J. Virol. **79**:8698–8706.
24. **Poh MK, Shui G, Xie X, Shi PY, Wenk MR, Gu F.** 2012. U18666A, an intra-cellular cholesterol transport inhibitor, inhibits dengue virus entry and replication. Antiviral Res. **93**:191–198.
25. **Byrd CM, Bolken TC, Mjalli AM, Arimilli MN, Andrews RC, Rothlein R, Andrea T, Rao M, Owens KL, Hruby DE.** 2004. New class of orthopoxvirus antiviral drugs that block viral maturation. J. Virol. **78**:12147–12156.
26. **Blaney JE, Jr, Hanson CT, Hanley KA, Murphy BR, Whitehead SS.** 2004. Vaccine candidates derived from a novel infectious cDNA clone of an American genotype dengue virus type 2. BMC Infect. Dis. **4**:39. doi:10.1186/1471-2334-4-39.
27. **Vrolijk JM, Kaul A, Hansen BE, Lohmann V, Haagmans BL, Schalm SW, Bartenschlager R.** 2003. A replicon-based bioassay for the measurement of interferons in patients with chronic hepatitis C. J. Virol. Methods **110**:201–209.
28. **Johnson AJ, Roehrig JT.** 1999. New mouse model for dengue virus vaccine testing. J. Virol. **73**:783–786.

29. **Kyle JL, Beatty PR, Harris E.** 2007. Dengue virus infects macrophages and dendritic cells in a mouse model of infection. J. Infect. Dis. **195**:1808–1817.
30. **Shresta S, Kyle JL, Snider HM, Basavapatna M, Beatty PR, Harris E.** 2004. Interferon-dependent immunity is essential for resistance to primary dengue virus infection in mice, whereas T- and B-cell-dependent immunity are less critical. J. Virol. **78**:2701–2710.
31. **Halstead SB.** 1988. Pathogenesis of dengue: challenges to molecular biology. Science **239**:476–481.
32. **van der Schaar HM, Rust MJ, Chen C, van der Ende-Metselaar H, Wilschut J, Zhuang X, Smit JM.** 2008. Dissecting the cell entry pathway of dengue virus by single-particle tracking in living cells. PLoS Pathog. **4**:e1000244. doi:10.1371/journal.ppat.1000244.
33. **Ma L, Jones CT, Groesch TD, Kuhn RJ, Post CB.** 2004. Solution structure of dengue virus capsid protein reveals another fold. Proc. Natl. Acad. Sci. U. S. A. **101**:3414–3419.
34. **Samsa MM, Mondotte JA, Iglesias NG, Assuncao-Miranda I, Barbosa-Lima G, Da Poian AT, Bozza PT, Gamarnik AV.** 2009. Dengue virus capsid protein usurps lipid droplets for viral particle formation. PLoS Pathog. **5**:e1000632. doi:10.1371/journal.ppat.1000632.
35. **Barba G, Harper F, Harada T, Kohara M, Goulinet S, Matsuura Y, Eder G, Schaff Z, Chapman MJ, Miyamura T, Brechot C.** 1997. Hepatitis C virus core protein shows a cytoplasmic localization and associates to cellular lipid storage droplets. Proc. Natl. Acad. Sci. U. S. A. **94**:1200–1205.
36. **Shavinskaya A, Boulant S, Penin F, McLauchlan J, Bartenschlager R.** 2007. The lipid droplet binding domain of hepatitis C virus core protein is a major determinant for efficient virus assembly. J. Biol. Chem. **282**:37158–37169.
37. **National Research Council of the National Academies.** 2011. Guide for the care and use of laboratory animals, 8th ed. National Academies Press, Washington, DC.